



Continuous fluorometric method for measuring β -Glucuronidase activity: comparative analysis of three fluorogenic substrates

Journal:	<i>Analyst</i>
Manuscript ID:	AN-ART-05-2015-001021.R1
Article Type:	Paper
Date Submitted by the Author:	20-Jul-2015
Complete List of Authors:	Regan, Fiona; Dublin City University, Chemical Sciences Briciu-Burghina, Ciprian; Dublin City University,, Chemical Sciences Heery, Brendan; Dublin City University,, Chemical Sciences

Cite this: DOI: 10.1039/c0xx00000x

www.rsc.org/xxxxxx

ARTICLE TYPE

Continuous fluorometric method for measuring β -Glucuronidase activity: comparative analysis of three fluorogenic substrates†

Ciprian Briciu-Burghina,^a Brendan Heery^a and Fiona Regan^{*a}

Received (in XXX, XXX) Xth XXXXXXXXX 20XX, Accepted Xth XXXXXXXXX 20XX

DOI: 10.1039/b000000x

E. coli β -Glucuronidase (GUS) activity assays are routinely used in fields such as plant molecular biology, applied microbiology and healthcare. Methods based on the optical detection of GUS using synthetic fluorogenic substrates are widely employed since they don't require expensive instrumentation and are easy to perform. In this study three fluorogenic substrates and their respective fluorophores were studied for the purpose of developing a continuous fluorometric method for GUS. The fluorescence intensity of 6-chloro-4-methyl-umbelliferone (6-CMU) at pH 6.8 was found to be 9.5 times higher than that of 4-methyl umbelliferone (4-MU) and 3.2 times higher than the fluorescence of 7-hydroxycoumarin-3-carboxylic acid (3-CU). Michaelis-Menten kinetic parameters of GUS catalysed hydrolysis of 6-chloro-4-methyl-umbelliferyl- β -D-glucuronide (6-CMUG) were determined experimentally ($K_m = 0.11$ mM, $K_{cat} = 74$ s⁻¹, $K_{cat}/K_m = 6.93 \times 10^5$ s⁻¹M⁻¹) and compared with the ones found for 4-methyl-umbelliferyl- β -D-glucuronide (4-MUG) ($K_m = 0.07$ mM, $K_{cat} = 92$ s⁻¹, $K_{cat}/K_m = 1.29 \times 10^6$ s⁻¹M⁻¹) and 3-carboxy-umbelliferyl- β -D-glucuronide (3-CUG) ($K_m = 0.48$ mM, $K_{cat} = 35$ s⁻¹, $K_{cat}/K_m = 7.40 \times 10^4$ s⁻¹M⁻¹). Finally a continuous fluorometric method based on 6-CMUG as a fluorogenic substrate has been developed for measuring GUS activity. When compared with the highly used discontinuous method based on 4-MUG as a substrate it was found that the new method is more sensitive and reproducible (%RSD=4.88). Furthermore, the developed method is less laborious, faster and more economical and should provide an improved alternative for GUS assays and kinetic studies.

Introduction

β -Glucuronidase (EC 3.2.1.31) enzymes catalyze the hydrolysis of β -D-glucopyranosiduronic derivatives into their corresponding aglycons and D-glucuronic acid sugar moieties. β -Glucuronidase (GUS) is a globular protein, active as a homotetramer and made up of 603 amino acids.¹ The enzyme is active as a homotetramer because the active sites contain elements of two neighbouring monomers, as revealed by the crystal structure (Scheme 1).² The active site residues of the enzyme are highly conserved. GUS enzyme retains the anomeric configuration of the glucuronic acid and is appropriately termed a retaining hydrolase.³ The enzyme has three important residues that participate in the break-down of glucuronides. It breaks down the O-glycosyl bond by nucleophilic attack with the nucleophilic residue being Glu504 (equivalent to Glu540 in humans). The acid-base residue is Glu413 (equivalent to human Glu451) while the residue Tyr468 (Tyr504 in humans) has been proven important but its role is not clear.^{3,4} Matsumura and Ellington⁵ modelled the *Escherichia coli* (*E. coli*) GUS against the human crystal structure and proposed that seven conserved residues (Asp163, Tyr468, Glu504, Tyr549, Arg562, Asn566 and Lys568) form eight intermolecular hydrogen bonds with the substrate. This bonding is thought to confer the typical specificity of GUS to β -D-glucuronide based

substrates. In a more recent study, Wallace *et al.* determined the crystal structure of bacterial GUS and when they aligned the sequence of *H. sapiens* GUS with the *E. coli* GUS they found a 45% sequence identity between the two. Furthermore they discovered the *E. coli* GUS contains a 17-residue "bacterial loop" which is not found in the human ortholog and they used this for selecting GUS inhibitors in the gastro intestinal tract.²

GUS enzymes have been found in animals, plants and microbes and their function and characteristics are subject to intensive studies in fields such as human healthcare, biology, microbiology and environmental monitoring.⁶ GUS *in-vitro* assays are extensively performed in various fields. In plant molecular biology, the GUS gene from *E. coli* is widely used as a reporter gene for the study of gene regulation in transformed plants.⁷ Gene expression in cells and tissue of transgenic plants is routinely studied using the GUS fusion system.^{8,9} GUS assays are routinely used for diagnostic purposes but also for specific detection of *E. coli* in water and food samples. When tested, GUS-positive reactions were observed in 94-96% of *E. coli* isolates.¹⁰⁻¹² GUS has been exploited as a marker enzyme for *E. coli* by the implementation of GUS targeted substrates into growth media.¹³ In this approach, the target bacteria are selectively grown and GUS activity is used as a confirmatory step. Direct measurement of GUS activity, without the culturing

Cite this: DOI: 10.1039/c0xx00000x

www.rsc.org/xxxxxx

ARTICLE TYPE

X

Scheme 1 Fluorogenic synthetic substrates investigated in this study (left) and their respective fluorophores (right) as hydrolysed by GUS. Crystal structure of the *E. coli* GUS tetramer² (middle) rendered with PyMOL (PDB ID: 3k46).

of target bacteria has also been used.¹⁴ In this case, the detection relies on measuring in-vitro GUS activity and the procedure is much quicker (3-4 h) and relatively easy to perform.¹⁴ The numerous applications mentioned above demonstrate the importance of developing a simple, sensitive, reliable and high-throughput method for measuring GUS activity. Methods based on optical detection of GUS activity are particularly attractive since they don't require expensive instrumentation and they are easy to perform routinely. For this purpose synthetic substrates made up of glucuronides linked to a chromophore or fluorophore have been designed for GUS.¹⁵ Colour formation or fluorescence due to the hydrolysis of the synthetic substrates can be recorded. In general, chromogenic substrates are phenol-based, water soluble, heat stable and specific and occur in a wide range of different colours.¹⁵ Although a few chromogenic substrates have been used for GUS, the use of fluorogenic substrates is more appealing. Fluorescence based techniques are usually 1000-fold more sensitive than absorbance based ones, since the detection is performed in the absence of light. The most common fluorogenic substrate is 4-methyl-umbelliferyl- β -D-glucuronide (4-MUG) which, upon hydrolysis, releases the fluorescent aglycon 4-methyl umbelliferone (4-MU) (Scheme 1).¹⁶ The major drawback of 4-MU is its high pKa value of 7.8, which causes only partial dissociation at pHs around the optimum pH for GUS activity. To overcome this issue, researchers have employed discontinuous enzyme assays which require the addition of alkali. This has the dual purpose of increasing the pH and of stopping the reaction due to GUS deactivation.⁷ Discontinuous assays have certain limitations when compared to continuous ones. For example, the continuous methods offer a more straightforward approach, where instant visualisation of the kinetic data enables prompt evaluation of the assay. Also, reagent consumption is minimised together with sample manipulation. Continuous absorbance¹⁷ and fluorescence¹⁸ based methods for measuring GUS activity exist; however, they are limited and cannot be applied when only small quantities of GUS are available.

In recent years new synthetic substrates developed previously are becoming commercially available. Among them, 3-carboxy-umbelliferyl- β -D-glucuronide (3-CUG) has been recently applied for the detection of *E. coli* GUS in a rugged *in-situ* optical sensor.¹⁹ The author reports a higher fluorescence and solubility of the new fluorophore compared with 4-MU in cold water. Another substrate, 6-chloro-4-methyl-umbelliferyl- β -D-glucuronide (6-CMUG) which enabled higher sensitivity at physiological pH is reported in the literature²⁰ and it was evaluated for the detection of *E. coli* in a culture based assay.²¹

In this context, we describe the development of an efficient

continuous fluorometric method for measuring *E. coli* GUS activity. This has been achieved by comparing two relatively new fluorogenic substrates (6-CMUG, 3-CUG) and their aglycons with the universally used 4-MUG (Scheme 1). The spectroscopic characteristics of the three substrates and their corresponding aglycons are analysed and compared and eventually the emission/excitation wavelengths are tuned to maximise the performance of the method at physiological pHs. We then evaluate the performance of the newly developed method against the widely used discontinuous one described by Jefferson⁷ and we show a better sensitivity and reproducibility can be achieved. Although the present work describes a continuous fluorometric method for measuring *E. coli* GUS activity, the current substrates and data may have application to analysis of GUS enzymes from various other sources.

Material and Methods

Materials

E. coli β -Glucuronidase type VII-A (27% purity), sodium phosphate monobasic and dibasic, sodium carbonate, sodium bicarbonate, sodium citrate, citric acid, 1,4- dithiothreitol (DTT), 7-hydroxyxoumarin-3-carboxylic acid (3-CU) (99%), 4-methyl umbelliferone (4-MU) (99%) and 4-methyl-umbelliferyl- β -D-glucuronide (4-MUG) (99%) were all purchased from Sigma Aldrich Ireland. The other two fluorogenic substrates 6-chloro-4-methyl-umbelliferyl- β -D-glucuronide (6-CMUG) (97%) and 3-carboxy-umbelliferyl- β -D-glucuronide (3-CUG) (99%) were ordered from Glycosynth Limited (UK) and Marker Gene Technologies (US), respectively. 6-chloro-4-methyl-umbelliferone (6-CMU) (97%) was ordered from Carbosynth Limited (UK). Water was passed through a Milli-Q water purification system.

Buffers were prepared fresh daily from stock solutions, sterilised by autoclaving at 115°C (200 kPa) for 15 min. pH studies involving GUS reaction rates, pKa calculations and excitation/emission optimisation were performed in a range of buffers at 50 mM spanning from pH 3.0 to 10.6 (Table S-1, ESI†). Buffer pH was measured using a Hanna Instruments pH meter with an accuracy of ± 0.01 pH units.

Stock solutions of fluorophores and substrates (100 mM) were prepared in 1 mL DMSO (99.5%) and kept at 4°C. Further dilutions were prepared daily in buffer or deionised water with a final DMSO concentration in the working solution, ranging from 0.01% -1%. GUS working solutions were kept on ice for the duration of the experiment and were prepared daily from stocks (1 mg mL⁻¹ stored at -20°C).

Methods

UV/Vis Spectroscopy

UV/Vis absorption spectra were obtained using a Shimadzu UV-1800 spectrophotometer. All spectra were obtained in the wavelength region spanning from 280 to 700 nm, using a 1 nm data interval.

Fluorescence spectroscopy

Fluorescence measurements were performed using two instruments. The first was an LSB 50 luminescence spectrometer from Perkin-Elmer equipped with Monk-Gillieson type adjustable monochromators and a gated photomultiplier tube. The light source was pulsed Xe, producing an output of 9.9 watts. The spectrofluorometer provides automatic correction of excitation spectra for wavelength dependent variations in the exciting lamp intensity. The second instrument was a Jasco FP 8300 Spectrofluorometer equipped with a holographic concave grating in modified Rowland mount monochromator and a 150 watts Xe lamp. A Peltier thermostatted single cell holder (ETC-273T) was used to maintain constant temperatures and for temperature studies. Sample cells were 3.5 mL (10x10 mm) and 1.4 mL (10x4 mm) UV quartz cuvettes, equipped with a Teflon stopper (Helma Analytics). Unless otherwise stated all the emission and excitation spectra were recorded using the accumulation mode as an average of 3 scans (with a scan speed of 200 nm min⁻¹). Most of the data presented was obtained using the Jasco FP 8300 instrument, unless otherwise stated in the legend.

Kinetic analysis (Michaelis-Menten Model)

Kinetic constants K_m and V_{max} were determined at pH of 6.8 ± 0.02 . Reaction velocities were determined at substrate concentrations ranging below and above K_m for each of the substrates. Substrate solutions of varying concentrations were prepared in 50 mM sodium phosphate buffer (pH 6.8) and brought to 20°C through incubation. Over the course of the experiments room temperature was recorded and it was maintained between 19.5–20 °C (± 0.1). Briefly 2.0 mL of the substrate solution was added to the cuvette, allowed to equilibrate and introduced into the fluorometer (set to time-drive acquisition mode). At this time a background reading of the fluorescence intensity was recorded, setting the excitation and emission maximum as determined for each of the substrates. A 10 μ L buffered GUS enzyme solution (0.1 mg mL⁻¹), kept on ice for stability, was added and the cuvette was vigorously mixed. The reaction was monitored by recording the increase in fluorescence intensity with readings taken every 5 s. The conversion from FU to actual product released/time unit was carried out through the use of calibration curves prepared for each fluorophore at each substrate concentration.

Temperature optimisation

GUS activity was measured using 6-MUG (0.5 mM), 3-CUG (1 mM) and 4-MUG (0.5 mM) at different temperatures, spanning from 6°C up to 70°C. The enzyme concentration was kept constant for the duration of the study (0.2 μ g mL⁻¹) and the measurement was performed in a continuous fashion. Briefly, 20 μ L GUS (0.01 mg mL⁻¹) was injected into 1.4 mL quartz cuvette containing 0.98 mL buffered substrate solution (pH 6.8) initially warmed/chilled to the desired temperature. The solution was vigorously mixed and placed in the fluorometer where the fluorescence was monitored using the λ_{ex} and λ_{em} maximum of each fluorophore. Measurements were collected every second for

60 6 min. Reaction rates (FU min⁻¹) were determined using the slope of fluorescence formation after normalisation to 1 min. In the case of high temperatures (50–70°C), where GUS denaturation was observed, slopes were determined only from the linear part of the data (1–4 min). To convert FU min⁻¹ into μ M min⁻¹ calibration curves were constructed for each of the three fluorophores, at 20°C using the same instrument settings and conditions as for the progress curves. Corrections to account for the fluorescence dependence on temperature were applied to the final data. An example on how the data was collected for the correction process is presented in Fig. S-10 ESI† for 3-CU. The same methodology was used for 4-MU and 6-CMUG. For each temperature and substrate a control was run without GUS to correct for the auto-hydrolysis of substrate during the assay period.

pH optimisation

For pH optimisation, reaction rates were determined using a discontinuous method adapted from Jefferson.⁷ Briefly 20 μ L GUS (0.025 mg mL⁻¹) was mixed with 0.98 mL buffered substrate (various pH values, Table S-1, ESI†) at room temperature, into 1.5 mL Eppendorf test tubes. After mixing the reaction was allowed to equilibrate and achieve maximum velocity for 1 min, when the first 100 μ L were collected into Eppendorf tubes containing 0.9 mL stop buffer (200 mM Na₂CO₃, pH 11.4). This was the “time=0” point, and successive 100 μ L aliquots were removed at regular time intervals (3, 6, 9 and 12 min). GUS activity (μ M min⁻¹) was determined through calibration curves of the three fluorophores in stop buffer and in the presence of substrate. All the experiments were performed in triplicate and a control without GUS was maintained.

Analytical performance of the continuous method

To assess the analytical performance of the continuous method described in this paper we used the widely known discontinuous method described by Jefferson⁷ as a comparison standard. The same concentration of GUS (5 ng mL⁻¹) was run for 10 times using both methods. Temperature was kept constant at 37°C and in both methods the reaction was allowed to proceed for 12 min. For the discontinuous method we used the same procedure as described above with the exception that the buffer pH was 6.8. In both methods the same settings were used on the fluorometer to facilitate direct comparison of the fluorescent signal.

Results and discussion

UV Vis characterisation of substrates and fluorophores

A preliminary study was carried out to investigate the absorption characteristics of substrates and fluorophores at different pH values in different buffers. Absorption spectra of substrates and fluorophores were recorded in acidic, neutral and alkaline conditions and are shown in Fig. 1. 4-MUG and 6-CMUG absorption spectra are not influenced by pH in the analysed range and are characterised by absorption bands centred at 318 nm for 4-MUG and 323 nm for 6-CMUG. On the other hand 3-CUG absorption band shifts from 329 nm (neutral and basic pH) to 342 nm (acidic pH). At pH 3.0, 3-CU shows the same absorption behaviour as 3-CUG (Fig. 1), with the same absorption band shift (13 nm) from 339 nm to 352 nm. This suggests that in both cases the same transition takes place which is the protonation of 3-carboxylate anion at pH values below 5.²²

Cite this: DOI: 10.1039/c0xx00000x

www.rsc.org/xxxxxx

ARTICLE TYPE

X

Fig. 1 Absorbance spectra of substrates (100 μM) and fluorophores (50 μM) in acidic, neutral and alkaline conditions; 4-MU/4-MUG (left), 6-CMU/6-CMUG (middle) and 3-CU/3-CUG (right). Legend applies to all the 3 panels. Absorption bands assigned to the N, A⁻ and A²⁻ are highlighted by the black arrows.

Contrarily to substrates, the fluorophores have absorption spectra which are pH dependent. The change in the absorption spectra can be explained by acid-base equilibrium due to the transition from the undissociated (neutral, N) to dissociated (anionic, A⁻) form with increasing pH (Fig. 1,4).

Extensive studies have been carried out on 4-MU and other coumarin derivatives, to better understand their ground and excited state properties. The fluorescence behaviour of 4-MU has been studied previously in organic solvents and in neutral, acidic and alkaline aqueous solutions.²³⁻²⁷ Moriya studied the ground and excited-state reactions of umbelliferone and 4-MU in acidic, neutral and alkaline conditions and concluded that in the electronic ground-state only two molecular species are spectroscopically detectable.²³ One is a neutral species (N) and the other is an ionized species (A⁻). If the pH is changed from acidic to basic the molecule is deprotonated at the 7-hydroxyl group. Later, the same author discovered the absorption band corresponding to the cationic species (C⁺) by conducting studies in concentrated sulphuric acid ($\lambda_{\text{max}} = 345 \text{ nm}$). The absorption λ_{max} is increased in the following order: N < C⁺ < A⁻.²⁸ The results of this study are consistent with those previous results and in the pH range tested only the N ($\lambda_{\text{max}} = 321 \text{ nm}$) and A⁻ ($\lambda_{\text{max}} = 364 \text{ nm}$) forms were detected for 4-MU in acidic and alkaline conditions. For 6-CMU a similar behaviour dictated by acid-base equilibrium with the 2 forms, N ($\lambda_{\text{max}} = 329 \text{ nm}$) and A⁻ ($\lambda_{\text{max}} = 369 \text{ nm}$) was observed. 3-CU on the other hand behaves slightly different in the pH range tested (Fig. 1). Due to the 3-carboxylic group, two protonation steps occur from basic to acidic pH.²² The band for the neutral form N is positioned at 352 nm. The A⁻ formed due to the deprotonation of the carboxy group appears at $\lambda_{\text{ex}} = 339 \text{ nm}$, while the dianionic form (A²⁻), after the second step deprotonation of the 7-hydroxy group is red shifted and appears at $\lambda_{\text{ex}} = 385 \text{ nm}$ (Fig. 1, 4).

X

Fig. 2 Spectrophotometric titration of the ground state equilibrium for 4-MU (top), 3-CU (middle) and 6-CMU (bottom), 50 μM . Drop lines highlight the pKa values inferred from the nonlinear regression fitting of the experimental data to the Boltzman Sigmoidal model. For 3-CU (middle panel) only the 5-10 pH range was used. Measurements were collected at the corresponding λ_{max} (N, A⁻) for each fluorophore and are reported in the legend as Abs.

The pKa values for the ground state equilibrium were estimated using spectrophotometric titration followed by nonlinear regression fitting of the experimental data to the Boltzman Sigmoidal model (Fig. 2). Experimental pKa values were found

to be: 7.86 ± 0.6 , $R^2 = 0.993$ (4-MU), 6.12 ± 0.3 , $R^2 = 0.996$ (6-CMU) and 7.38 ± 0.6 , $R^2 = 0.993$ (3-CU). These values are similar to the ones reported in the literature for 4-MU²⁹ and 3-CU³⁰ while for 6-CMU, no pKa value is reported. The low pKa value of 6-CMU makes this fluorophore ideal for fluorometric assays at physiological pH values, as it is almost fully dissociated into the anion at this pH.

Fluorometric characterisation of substrates and fluorophores

As 3-CU^{30,31} and 6-CMU²⁰ have been synthesised more recently than 4-MU, there is a lack of literature on the behaviour of these two fluorophores in the ground and excited state. Excitation and emission 3D scans of 4-MU, 3-CU and 6-CMU in different buffers and at different pH values ranging from 3.0 up to 11.0 were collected. Analysis of the emission spectra over the pH range revealed that the shape of the emission spectrum is pH and excitation wavelength independent. The emission maximum (λ_{em}) was found to be 447 nm for 4-MU, 445 nm for 3-CU and 452 nm for 6-CMU, respectively (Fig. 3). Although in the ground state the studied fluorophores show two spectroscopically detectable species, in the excited state only one form was detected, corresponding to the λ_{em} for each. When excited at different wavelengths, the fluorophores yield the same emission spectrum over the pH range tested, regardless of which ground state species absorbs the excitation energy. Previous studies on 4-MU and umbelliferone conjugates have shown that there are actually 4 excited state possible species depending on pH and solvent: enol or neutral (N*), anion (A*), cation (C*) and a long-wave emitting keto-tautomeric form (K*).^{28, 29, 32} The tautomeric form is an excited state reaction product due to proton transfer between the spatially separated acidic (OH) and basic (C=O) groups. The fact that only the A* (4-MU, 6-CMU) and A²⁻* (3-CU) were detected in the excited state is a consequence of a dissociative process in the excited state. Therefore the neutral excited molecule in the solution is converted in its lifetime into the anionic form and emits at the same wavelength as the anionic excited molecule.²³ This process is better known as the Kasha's rule.

Excitation spectra were collected by setting the emission wavelength at the λ_{em} for each of the three fluorophores and results are reported in Fig. 4. There is a striking similarity between the excitation and absorption spectra for each of the fluorescent molecules. The absorption and excitation spectra are practically super imposable. This allows for the assignment of the absorbing species in the ground state to the same species that absorb the excitation energy.³³ Upon increase of the pH from 3.0 to 11.5 the excitation band corresponding to the N form gradually

Cite this: DOI: 10.1039/c0xx00000x

www.rsc.org/xxxxxx

ARTICLE TYPE

X

Fig. 3 Emission spectra of 2.46 μM 3-CU (left), 4-MU (middle) and 6-CMU (right) in acidic, neutral and alkaline conditions at 20°C. λ_{ex} denoted in the legend (in brackets) were used to collect the corresponding emission spectra. The same instrument configuration was used for all measurements.

X

Fig. 4 Excitation spectra of 2.46 μM 3-CU (3-CU), 4-MU (middle) and 6-CMU (bottom) at 20°C in the 3.0- 11.5 pH range. λ_{em} used to collect the excitation spectra were 445 nm (3-CU), 447 nm (4-MU) and 452 nm (6-CMU). Dotted arrows in the top panel highlight the appearance of the A²⁻ (pH 4.0, 3.6, 3.0) in the case of 3-CU. Insets show the pH dependent emission of 2.46 μM 3-CU (3-CU), 4-MU (middle) and 6-CMU (bottom) at 20°C in the pH range tested while the dotted drop lines highlight the intensity at pH 6.8; λ_{ex} used for each fluorophore are mentioned in the legend. The same instrument configuration was used for all the measurements.

decreases being replaced with a new excitation band corresponding to the A⁻ form. This is the case for 4-MU and 6-CMU, while for 3-CU there is a deviation from this model due to the two step dissociation of the hydroxy and carboxy groups. The isosbestic points at 347 nm (3-CU), 333 nm (4-MU) and 337 nm (6-CMU) indicate the ground state equilibrium between the A²⁻ and A⁻ form for 3-CU and the N and A⁻ form for 4-MU and 6-CMU (Fig. 4).

Emission spectra were collected by setting the excitation wavelength corresponding to the maximum bands found for the A⁻ forms for 4-MU and 6-CMU and for the A²⁻ form for 3-CU. Fluorescence intensities recorded at the maximum emission wavelength for each fluorophore were plotted against pH. The fluorescence intensity of 6-CMU in the 6.8-7.0 pH range was found to be roughly 9.5 times higher than that of 4-MU and 3.2 times higher than the fluorescence of 3-CU (Fig. 4 inset). This further proves, that the low pKa value of 6-CMU renders this fluorophore as a superior candidate for continuous measurements at physiological pH values. On the other hand, at pH values above 9 where full dissociation occurs, 3-CU emits a fluorescent signal 1.5 times higher than 4-MU and 1.3 times higher than 6-CMU, making 3-CU a better candidate for discontinuous measurements where the pH can be adjusted.

Continuous monitoring of GUS activity requires that changes in fluorescence intensity to be measured in the conditions of the reaction assay, where the fluorophore is produced in μM or nM concentration in a mM solution of substrate. Hence the effect of the presence of different substrate concentrations on the fluorescence spectra of fluorophores was investigated. It was found that the inner filter effect³⁴⁻³⁶ has a substantial impact on the optimal excitation wavelength and consequently on the intensity of emitted fluorescent signal. When the same concentration of fluorophore was used in the presence of increasing concentrations of substrates (0-2 mM) at pH 6.8, a red shift of the maximum excitation wavelength (λ_{ex}) was noticed for

4-MU and 3-CU (Fig. 5). This shift is caused by the increasing absorbance of substrate with increasing concentration. As a consequence, 4-MU and 3-CU which at pH 6.8 have a maximum excitation wavelength at 321 nm and 339 nm due to the N form which is predominant were obstructed from absorbing incident light at shorter wavelengths. This is particularly important if enzyme assays are to be carried out at suboptimal substrate concentrations (around K_m value or lower) as the excitation wavelength can be chosen to maximise the fluorescent signal and by that the LOD and the sensitivity of the assay. When the same studies were performed for 6-CMU using different concentrations of 6-CMUG it was found that the substrate had no influence on the maximum excitation wavelength of the fluorophore. This is due to the lower pKa value of 6-CMU (6.18 \pm 0.3). At pH 6.8, 6-CMU is almost fully dissociated and absorbs strongly at 369 nm (Fig. 5).

A suitable method to continuously monitor GUS activity requires that the fluorescence of the fluorophore (reaction product) to be directly proportional to its concentration in the reaction medium. This also implies that the excitation wavelength for the fluorophore has to be chosen not only to confer linearity but also to maximise the LOD and the sensitivity of the method. For this purpose the concentration of substrate was kept constant at 0.5 mM and increasing concentrations of fluorophore were added. It was found that the presence of substrate does not influence the shape of the emission spectrum for any of the fluorophores, affecting only the intensity of the emitted fluorescence (Fig. S-1, S-2, S-3, ESI†).

80 Kinetic analysis of GUS catalysed hydrolysis of the substrates

One way to investigate the interaction between GUS and the three substrates: 4-MUG, 3-CUG and 6-CMUG is through the use of Michaelis Menten parameters: K_m and V_{max} . A comparison between these parameters for the three substrates can give insights into the enzyme's preferred molecule, catalysis rates and optimal substrate concentration. By conducting studies under the same conditions (pH, temperature and GUS concentration) a comparison and a decision can be made regarding which of these substrates is optimal for continuous GUS assay.

A study was conducted to investigate the Michaelis-Menten kinetic parameters between GUS and 4-MUG, 3-CUG and 6-CMUG. Fluorescence change is a convenient and sensitive approach to monitor kinetics of hydrolytic enzymes. Unfortunately, it loses linearity as the absorbance of the fluorogenic substrate increases with concentration increasing the IFE (inner filter effect). Decreases in fluorescence due to the inner filtering exceed 10% once the sum of absorbance at

Cite this: DOI: 10.1039/c0xx00000x

www.rsc.org/xxxxxx

ARTICLE TYPE

X

Fig. 5 Excitation spectra of 2.5 μM 3-CU (left), 4-MU (middle) and 6-CMU (right) in the presence of 3-CUG, 4-MUG and 6-CMUG at pH 6.8 and 20°C. Legend in the left panel applies to all the panels in the Fig. and it represents the molar concentrations of the substrates. Overlaid with dotted lines are the absorbance spectra of 3-CUG, 4-MUG and 6-CMUG at 100 μM at pH 6.8 and 20 °C. Horizontal arrows denote the λ_{ex} shift while vertical arrows denote the substrate concentration increase. Each substrate + fluorophore spectrum was corrected by subtracting the spectrum of the respective substrate concentration.

excitation and emission wavelengths exceed 0.08³⁷. To overcome this issue, corrections for absorbance are applied to the experimental data or calibration curves for the fluorophore are constructed in the presence of different substrate concentrations. The latter, although more laborious and time consuming than the former, will give more accurate estimations of the kinetic parameters. For this purpose calibration curves were performed for each substrate concentration using different fluorophore dilutions. Fig. S-4, S-5, S-6, ESI† show the calibration curves used to convert fluorescence units (FU) into μM concentration of product. The highest signal loss due to IFE and probably fluorescence quenching was noticed in the case of 4-MU followed by 3-CU and 6-CMU. This loss in the fluorescence efficiency of the fluorophore with increasing substrate concentration can introduce errors into the determination of kinetic parameters if it is not taken into account. Progress curves of fluorescence accumulation as a function of time were measured for each of the 3 substrates in the presence of GUS and are shown in Fig. S-7, S-8, S-9, ESI†. Equation (1) was used to calculate the initial velocities from the slope of the progress curves (Slope 2) and the slope of the fluorophores calibration curves (Slope 1).

$$\text{Initial velocity } (\mu\text{M min}^{-1}) = \frac{\text{Slope 2 (FU s}^{-1}) * 60}{\text{Slope 1 (FU } \mu\text{M}^{-1})} \quad (1)$$

$$V = \frac{V_{\text{max}}[S]}{K_m + [S]} \quad (2)$$

Initial reaction velocities were plotted against substrate concentration. Michaelis-Menten equation (2) was used to estimate the K_m and V_{max} using Solver. The model estimates the two parameters by minimising the sum of square residuals (SSR). A residual analysis was carried out for each of three models to determine if the model is a good fit for the data. Fig. 6 shows the best fit of the Michaelis-Menten model to the experimental data for 4-MUG, 3-CUG and 6-CMUG. K_m/V_{max} values derived from the 3 models are summarised in Table 1 together with the calculated K_{cat} values. As experiments were conducted under identical conditions and with similar enzyme concentrations, the Michaelis-Menten constants can be directly compared to identify possible binding preferences. The K_m value for 3-CUG is almost 7 times higher when compared with that obtained for 4-MUG and 4.5 times higher when compared to the K_m value for 6-CMUG. This suggests a preferential binding of GUS to 4-MUG and 6-CMUG which also suggests that a much lower concentration of

4-MUG and 6-CMUG is needed to maximise the reaction velocity. Maximum rate, V_{max} occurs when the intrinsic binding energy is used for the catalytic process rather than binding and is a result of the enzyme binding the substrate weakly but the transition state strongly. Maximum catalysis rates, K_{cat}/K_m , occur when the structure of the enzyme is complementary to the transition state of the substrate and the intrinsic binding energy is used to stabilise the transition state.³⁸ Our results show that 4-MUG has the highest first order catalysis rate (K_{cat}/K_m), followed by 6-CMUG and 3-CUG (Table 1). This suggests that the transition state structure of 4-MUG and 6-CMUG are more complementary to the enzyme binding site that the transition state of 3-CUG. Differences in binding preferences are commonly due to the steric differences or electronic hindrances at the enzyme binding site. Since the two catalytic residues in GUS are Glu413 and Glu504^{2, 39} it was proposed that the similarity between the active site and the 3-carboxyl group of the aglycon in 3-CUG might result in electronic repulsion, which translates into a lower affinity of the enzyme for the substrate and a higher Michaelis-Menten constant.⁴⁰ Using the K_m values derived from the Michaelis-Menten model one can calculate how much substrate is required to reach any desired level of saturation. For zero order reactions the substrate concentration is usually kept high (at least 3 times the K_m value).⁴¹ The kinetic parameters from Table 1 suggest that 4-MUG would be the preferred substrate of choice in assaying GUS activity, closely followed by 6-CMUG. On the other hand, the progress curves in Fig. S-7, S-9, ESI† show that

Table 1 Kinetic parameters for GUS.

Substrate	K_m (mM) ^a	V_{max} ($\mu\text{M min}^{-1}$) ^a	k_{cat} (s ⁻¹) ^a	k_{cat} (s ⁻¹) ^b	K_{cat}/K_m (s ⁻¹ M ⁻¹) ^a
4-MUG	0.07	2.56	92	222 ± 13.4	1.29 × 10 ⁶
3-CUG	0.48	0.99	35	132 ± 9.3	7.40 × 10 ⁴
6-CMUG	0.11	2.07	74	207 ± 8.5	6.93 × 10 ⁵

^a Measurements performed at 20°C and pH 6.8 with 135 ng mL⁻¹ GUS.

^b Measurements performed at 37°C and pH 6.8 with 1.35 ng mL⁻¹ GUS.

the same amount of GUS will produce a fluorescent signal 6 times higher in the presence of 6-CMUG as compared to 4-MUG. Taking this into account it is clear that a method based on 6-CMUG will have an improved LOD and better response times. To our knowledge this is for the first time Michaelis-Menten catalytic parameters are reported for the GUS hydrolysis of 6-CMUG. These studies suggest 6-CMUG is a suitable candidate for measuring *E. coli* GUS activity using a continuous fluorometric method.

Cite this: DOI: 10.1039/c0xx00000x

www.rsc.org/xxxxxx

ARTICLE TYPE

X

Fig. 6 Kinetics of GUS (135 ng mL^{-1}) catalysed hydrolysis of 3-CUG (left) 4-MUG (middle) and 6-CMUG (right) and nonlinear regression fitting of the experimental data to the Michaelis-Menten model. Initial reaction velocities were determined at 20°C and pH 6.8. The insets in each panel show the distribution of residuals for each run (V1, V2, and V3). Error bars represent the standard deviation of $n=3$.

5 Temperature and pH optimisation

Enzyme assays are carried out in well defined conditions for consistent and reproducible results. Temperature and pH play an important role in both the development of enzyme assays but also on the study of enzyme structures. Temperature influences enzyme catalysed reactions in the same way it influences other chemical reactions. As a general rule, reaction rates increase with temperature by a factor of 2-3 for each 10°C . Once the temperature exceeds a certain maximum value turnover rates start to decline due to destabilisation and deactivation of the enzyme.

Fig. 7 shows the temperature profile for GUS catalysed hydrolysis of 4-MUG, 6-CMUG and 3-CUG. Although maximum reaction rates were observed at 44°C (3-CUG and 6-CMUG) and 50°C (4-MUG) we chose to use 37°C as the optimum temperature to make sure GUS denaturation doesn't occur.⁴² Previous studies on wild type GUS using 4-nitrophenyl- β -D-glucuronide (4-NPG) and 4-MUG⁴³ as substrate^{44,45} and recombinant GUS using 3-CUG as substrate⁴⁰ report similar temperature profiles with a maximum activity between 40 - 50°C . Between 10 - 40°C GUS activity increased linearly with temperature, at a rate of 0.08 , 0.07 and $0.05 \mu\text{M min}^{-1} ^\circ\text{C}^{-1}$ for 4-MUG, 6-CMUG and 3-CUG respectively. Denaturation was observed after 50°C while above 65°C there was little or no activity left. Because a continuous method was used to determine GUS activity within the temperature range, a correction for the influence of temperature on the intensity of the three fluorophores was applied to calibration curves recorded at 20°C in the assay buffer (Equation in Fig. S-11, ESI†). In this case only one calibration curve was needed for each substrate. We found that there is a 15% loss in 6-CMU fluorescence with temperature rise (from 2°C to 70°C) which is normal in such systems and is due to the thermal activation of non-radiative de-excitation pathways.⁴⁶ On the other hand, for 4-MU and 3-CU a 60% and 40% gain in fluorescence was noticed for the same temperature interval (Fig. S-11, ESI†). These two fluorophores have a higher pK_a than 6-CMU and are just partially dissociated at pH 6.8. With increasing temperature the equilibrium is shifted to the right thus decreasing the pK_a and favouring the dissociation process. This process is explained by excitation spectra collected for the three fluorophores in the 5 - 70°C temperature range (Fig. S-12, ESI†) where the absorption bands corresponding to the A^- (4-MU) and A^{2-} (3-CU) are gradually increasing with temperature.

The pH profile plays an important role in the activity of enzymes because it is responsible for the ionization of functional groups directly involved in catalysis and any charged groups involved in the stabilisation of the protein structure. As a consequence the pH dependence can offer insight into the

catalytically active functional groups and potentially their chemical nature. In the case of GUS the activity increases with pH to a maximum (pH 6.6 -7.2) and drops to zero in the alkaline region following a bell shaped curve (Fig. 7). Similar pH optimum values for *E. coli* GUS activity are reported in the literature in the presence of various substrates and range from 6.5 up to 7.5 pH units.^{44,43,47,48,49,50} This behaviour is consistent with a simple diprotic system where the increase and decrease in activity on both sides of the optimum pH represents titration curves of active site residues. The midpoints on the curves correspond to the pK values of these active groups in the enzyme substrate complex.⁴² Our results suggest that there is no difference between the pH profiles with the three substrates (Fig. 7). This confirms that the shape of the pH curve is driven by functional groups in GUS and not by functional groups in the substrate.

X

Fig. 7 Temperature (left) and pH (right) profiles for GUS catalysed hydrolysis of 3-CUG (2 mM), 4-MUG (0.5 mM) and 6-CMUG (0.5 mM). pH profiles were recorded at 20°C in the presence of 135 ng mL^{-1} GUS while temperature profiles were recorded at pH 6.8 in the presence of 54 ng mL^{-1} GUS. Error bars represent the standard deviation of $n=3$.

Analytical performance of the continuous method

Results presented in the previous sections suggest that 6-CMUG is the preferred substrate for measuring GUS activity in a continuous fashion. To further test this, the continuous fluorometric method developed in this study was compared with the widely used discontinuous method⁷ based on 4-MUG. The same GUS concentration was run 10 times using both methods (Fig. 8). The average activity was found to be $0.041 \pm 0.0025 \mu\text{M min}^{-1}$ (4-MUG) and $0.058 \pm 0.0028 \mu\text{M min}^{-1}$ (6-CMUG) with a %RSD of 6.20 and 4.88 respectively. The smaller %RSD for the continuous method is expected and is probably due to fewer random errors introduced during the experimental procedure. The discontinuous method is more susceptible to such errors due to the multiple handling steps required and this aspect is also noticeable from the linear fitting of the experimental data (Fig. 8). The difference in the two average activities is significant and is likely due to GUS loss during the process. Since, for this experiment, we used a relatively low GUS concentration, it is likely that the multiple pipetting steps required for the discontinuous method are the underlying cause of this observation. For the same GUS concentration the continuous method offers an almost 10 fold improvement in the fluorescent signal recorded (note the scale in Fig. 8). This is due to the inherent disadvantage of the discontinuous method which

Cite this: DOI: 10.1039/c0xx00000x

www.rsc.org/xxxxxx

ARTICLE TYPE

X

Fig. 8 Comparison of the discontinuous (top) and continuous (bottom) method for measuring GUS activity. Progress curves (normalised to $t=0$ min) from running the same GUS concentration (1.35 ng mL^{-1}) 10 times with the two methods (middle), emission spectra as a function of time (left) and box plots after conversion (right). For the 4-MUG based method GUS activities were multiplied by 10 to account for the dilution factor. Emission spectra in the left panel were collected at 3 min intervals (discontinuous method) and at 2 min intervals (continuous method). Insets in the left panel show images collected for both methods before and 12 min after GUS addition. Experimental conditions are detailed in Methods section

requires the measurement of fluorophore produced in a 10 fold dilution. Although 4-MU is slightly more fluorescent at pH 10.6 than 6-CMU at pH 6.8, the requirement for stopping the enzymatic reaction with concomitant pH adjustment and dilution results in an increase in the LOD of the discontinuous method. Besides the analytical capabilities, the continuous method offers other advantages such as time and labour savings and is more sustainable with regard to reagents and consumables used. As an example, for the experimental data collected in Fig. 8, both methods required between 5-6 h to generate results but the effective working time was approximately 5 h for the discontinuous method and approximately 30 min for the continuous one. Furthermore, over 100 pipette tips and 76 test tubes were used, generating 55-60 mL of waste using the discontinuous method as opposed to 2 pipette tips and 11 mL of waste for the continuous method. When data are obtained in a discontinuous set-up, aliquots are removed at pre-determined times as the enzymatic reaction proceeds. The fluorescence is then measured and a progress curve is constructed ensuring the product formation proceeds linearly. This is not necessarily an easy task when it is considered that only a limited number of measurement points are available and deviations from linearity are often hard to identify. In a continuous set-up, once the enzymatic reaction has been initiated the product formation can be monitored at a higher rate. Deviations from linearity can be observed in real time and collected kinetic data is more accurate and offers a more detailed insight into the chemical process. GUS activity can be measured in less than 2 min as long as the linearity is checked and maintained. One disadvantage of the continuous method is that using a single cell holder bench fluorometer, only one sample can be analysed at any time while the discontinuous method allows for simultaneous analysis of multiple samples. This can be easily corrected if the 6-CMUG method is coupled with a plate reader. This set-up should also provide high-throughput screening of GUS activity. Although we developed this method for diagnostic purposes and particularly for the detection of *E. coli* in environmental water samples its applicability can be easily extended to other areas. GUS activity measurements are performed and routinely used in plant molecular biology, human healthcare, biology, microbiology and environmental monitoring⁶. Furthermore, the method can be easily automated and can eventually be employed in a flow-through system for unattended sample analysis and sensing applications.

Conclusions

In summary, two lesser known fluorogenic substrates (6-CMUG and 3-CUG) were studied and compared with the widely used 4-MUG for measuring GUS activity in a continuous set-up. Spectrophotometric characterization using UV Vis and steady state fluorescence spectroscopy of fluorophores and substrates revealed that 6-CMUG is the substrate of choice for continuous measurements. This was found to be mainly due to the lower pK_a value (6.12 ± 0.3) of its fluorophore 6-CMU. As a consequence, at pH 6.8 where GUS activity reaches its maximum this fluorophore is almost fully dissociated into its A^- form. When emission spectra were collected using the excitation bands for the ionised forms of 4-MU, 6-CMU and 3-CU, the fluorescence intensity of 6-CMU was found to be roughly 9.5 times higher than that of 4-MU and 3.2 times higher than the fluorescence of 3-CU. Michaelis-Menten kinetic parameters of GUS catalysed hydrolysis of 4-MUG, 3-CUG and 6-CMUG were determined experimentally and compared and are reported for the first time in case of 6-CMUG ($K_m = 0.11 \text{ mM}$, $K_{cat} = 74 \text{ s}^{-1}$, $K_{cat}/K_m = 6.93 \times 10^5 \text{ s}^{-1}\text{M}^{-1}$ at pH 6.8 and 20°C). Finally a continuous fluorometric method based on 6-CMUG as a fluorogenic substrate has been developed for measuring GUS activity. When compared with the highly used discontinuous method based on 4-MUG as a substrate it was found that the new method is more sensitive (almost 10 times) and more reproducible (%RSD=4.88). Furthermore, the developed method is less laborious, faster and more economical and should provide an improved alternative for GUS assays and GUS kinetic studies.

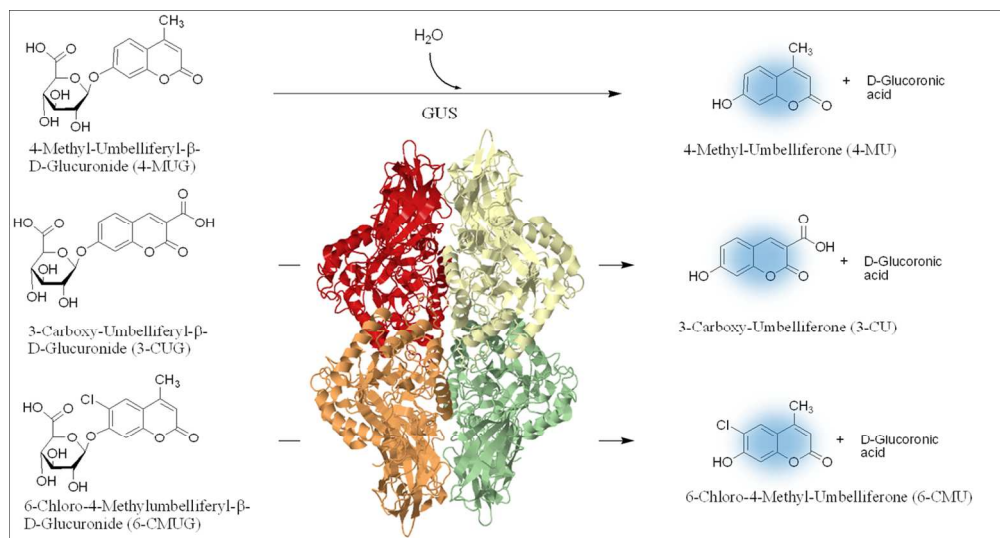
Acknowledgments

This work was funded under the EU Framework 7 project "ATWARM" (Marie Curie ITN, No. 238273) and by the Irish Research Council (IRC) under the Enterprise Partnership Scheme in collaboration with T.E. Laboratories, as part of the International SmartOcean Graduate Enterprise initiative (ISGEI).

Notes and references

- ^a Marine and Environmental Sensing Technology Hub (MESTECH), National Centre for Sensor Research (NCSR), School of Chemical Sciences, Dublin City University, Dublin, Ireland;
⁹⁰ E-mail: fiona.regan@dcu.ie

- † Electronic Supplementary Information (ESI) available: [1 table and 11 figures]. See DOI: 10.1039/b000000x/
‡ Footnotes should appear here. These might include comments relevant to but not central to the matter under discussion, limited experimental and spectral data, and crystallographic data.
- 1 B. Henrissat, *Biochem. J.*, 1991, **280**, 309.
2 B. D. Wallace, H. Wang, K. T. Lane, J. E. Scott, J. Orans, J. S. Koo, M. Venkatesh, C. Jobin, L. A. Yeh, S. Mani and M. R. Redinbo, *Science*, 2010, **330**, 831-835 (DOI:10.1126/science.1191175 [doi]).
3 M. R. Islam, S. Tomatsu, G. N. Shah, J. H. Grubb, S. Jain and W. S. Sly, *J. Biol. Chem.*, 1999, **274**, 23451.
4 A. W. Wong, S. He, J. H. Grubb, W. S. Sly and S. G. Withers, *J. Biol. Chem.*, 1998, **273**, 34057-34062.
5 I. Matsumura and A. D. Ellington, *J. Mol. Biol.*, 2001, **305**, 331-339.
6 L. J. Gilissen, P. L. Metz, W. J. Stiekema and J. Nap, *Transgenic Res.*, 1998, **7**, 157-163.
7 R. A. Jefferson, *Plant Mol. Biol. Rep.*, 1987, **5**, 387-405.
8 R. A. Jefferson, S. M. Burgess and D. Hirsh, *Proc. Natl. Acad. Sci. U. S. A.*, 1986, **83**, 8447-8451.
9 K. J. Wilson, S. Hughes and R. Jefferson, 1992, .
10 P. Feng and P. A. Hartman, *Appl. Environ. Microbiol.*, 1982, **43**, 1320-1329.
11 S. C. Edberg and C. M. Kontnick, *J. Clin. Microbiol.*, 1986, **24**, 368-371.
12 C. W. KASPAR and A. K. BENSON, 1987, .
13 A. Rompré, P. Servais, J. Baudart, M. de-Roubin and P. Laurent, *J. Microbiol. Methods*, 2002, **49**, 31-54.
14 L. Fiksdal and I. Tryland, *Curr. Opin. Biotechnol.*, 2008, **19**, 289-294.
15 E. Frampton and L. Restaino, *J. Appl. Microbiol.*, 2008, **74**, 223-233.
16 M. Manafi, *Int. J. Food Microbiol.*, 2000, **60**, 205-218.
17 S. Aich, *BioTechniques*, 2001, **30**, 846-851.
18 S. Fior, A. Vianelli and P. D. Gerola, *Plant science*, 2009, **176**, 130-135.
19 J. R. Geary, G. M. Nijak, S. L. Larson and J. W. Talley, *Enzyme Microb. Technol.*, 2011, **49**, 6-10.
20 K. Chilvers, J. Perry, A. James and R. Reed, *J. Appl. Microbiol.*, 2002, **91**, 1118-1130.
21 J. D. Perry, A. James, K. Morris, M. Oliver, K. Chilvers, R. Reed and F. Gould, *J. Appl. Microbiol.*, 2006, **101**, 977-985.
22 K. K. Sadhu, S. Mizukami, A. Yoshimura and K. Kikuchi, *Organic & biomolecular chemistry*, 2013, **11**, 563-568.
23 T. Moriya, *Bull. Chem. Soc. Jpn.*, 1983, **56**, 6-14.
24 D. Jacquemin, E. A. Perpète, G. Scalmani, M. J. Frisch, X. Assfeld, I. Ciofini and C. Adamo, *J. Chem. Phys.*, 2006, **125**, 164324.
25 J. P. Cerón-Carrasco, M. Fanuel, A. Charaf-Eddin and D. Jacquemin, *Chemical Physics Letters*, 2012, .
26 J. Seixas de Melo and P. Fernandes, *J. Mol. Struct.*, 2001, **565**, 69-78.
27 B. Cohen and D. Huppert, *The Journal of Physical Chemistry A*, 2001, **105**, 7157-7164.
28 T. Moriya, *Bull. Chem. Soc. Jpn.*, 1988, **61**, 1873-1886.
29 S. G. Schulman and L. S. Rosenberg, *J. Phys. Chem.*, 1979, **83**, 447-451.
30 W. Sun, K. R. Gee and R. P. Haugland, *Bioorg. Med. Chem. Lett.*, 1998, **8**, 3107-3110.
31 J. Chalom, C. Griffoul, M. Tod and S. Reveilleau, *Hydrosoluble coumarin derivatives, their preparation and their use as an enzyme substrate or for the preparation of such substrates*, 1994, .
32 I. Georgieva, N. Trendafilova, A. Aquino and H. Lischka, *The Journal of Physical Chemistry A*, 2005, **109**, 11860-11869.
33 D. W. Fink and W. R. Koehler, *Anal. Chem.*, 1970, **42**, 990-993.
34 M. Kubista, R. Sjöback, S. Eriksson and B. Albinsson, *Analyst*, 1994, **119**, 417-419.
35 M. O. Palmier and S. R. Van Doren, *Anal. Biochem.*, 2007, **371**, 43-51.
36 Q. Gu and J. E. Kenny, *Anal. Chem.*, 2008, **81**, 420-426.
37 E. D. Matayoshi, G. T. Wang, G. A. Krafft and J. Erickson, *Science (New York, NY)*, 1990, **247**, 954.
38 A. Fersht, *Proceedings of the Royal Society of London. Series B. Biological Sciences*, 1974, **187**, 397-407.
39 S. Jain, W. B. Drendel, Z. Chen, F. S. Mathews, W. S. Sly and J. H. Grubb, *Nature Structural & Molecular Biology*, 1996, **3**, 375-381.
40 J. R. Geary, G. M. Nijak Jr, S. L. Larson and J. W. Talley, *Enzyme Microb. Technol.*, 2011, **49**, 6-10.
41 J. Markwell, *Biochemistry and Molecular Biology Education*, 2009, **37**, 317-318.
42 A. Cornish-Bowden, *Fundamentals of enzyme kinetics*, John Wiley & Sons, 2013.
43 I. George, M. Petit and P. Servais, *J. Appl. Microbiol.*, 2000, **88**, 404-413.
44 A. S. Xiong, R. H. Peng, Z. M. Cheng, Y. Li, J. G. Liu, J. Zhuang, F. Gao, F. Xu, Y. S. Qiao, Z. Zhang, J. M. Chen and Q. H. Yao, *Protein Eng. Des. Sel.*, 2007, **20**, 319-325 (DOI:gzm023 [pii]).
45 H. Flores and A. D. Ellington, *J. Mol. Biol.*, 2002, **315**, 325-337.
46 X. Wang, O. S. Wolfbeis and R. J. Meier, *Chem. Soc. Rev.*, 2013, **42**, 7834-7869.
47 D. H. Kim, Y. H. Jin, E. A. Jung, M. J. Han and K. Kobashi, *Biol. Pharm. Bull.*, 1995, **18**, 1184-1188.
48 D. R. Witcher, E. E. Hood, D. Peterson, M. Bailey, D. Bond, A. Kusnadi, R. Evangelista, Z. Nikolov, C. Wooge and R. Mehigh, *Mol. Breed.*, 1998, **4**, 301-312.
49 S. Aich, L. T. Delbaere and R. Chen, *Protein Expr. Purif.*, 2001, **22**, 75-81.
50 J. R. Geary, G. M. Nijak, S. L. Larson and J. W. Talley, *Enzyme Microb. Technol.*, 2011, **49**, 6-10.



Scheme 1
254x135mm (150 x 150 DPI)

1
2
3
4
5
6
7
8
9
10
11
12
13
14
15
16
17
18
19
20
21
22
23
24
25
26
27
28
29
30
31
32
33
34
35
36
37
38
39
40
41
42
43
44
45
46
47
48
49
50
51
52
53
54
55
56
57
58
59
60

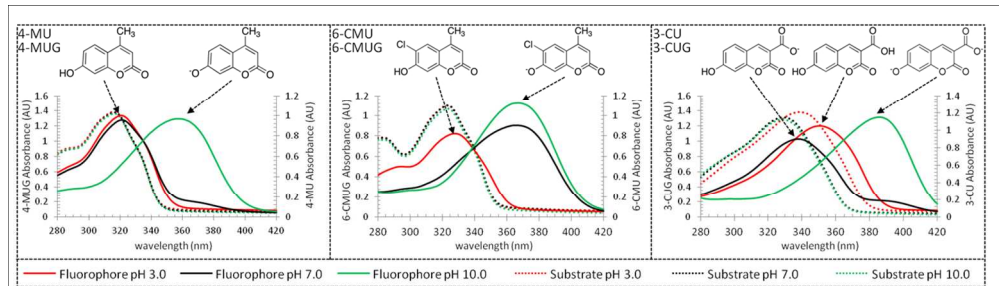


Figure 1
254x71mm (150 x 150 DPI)

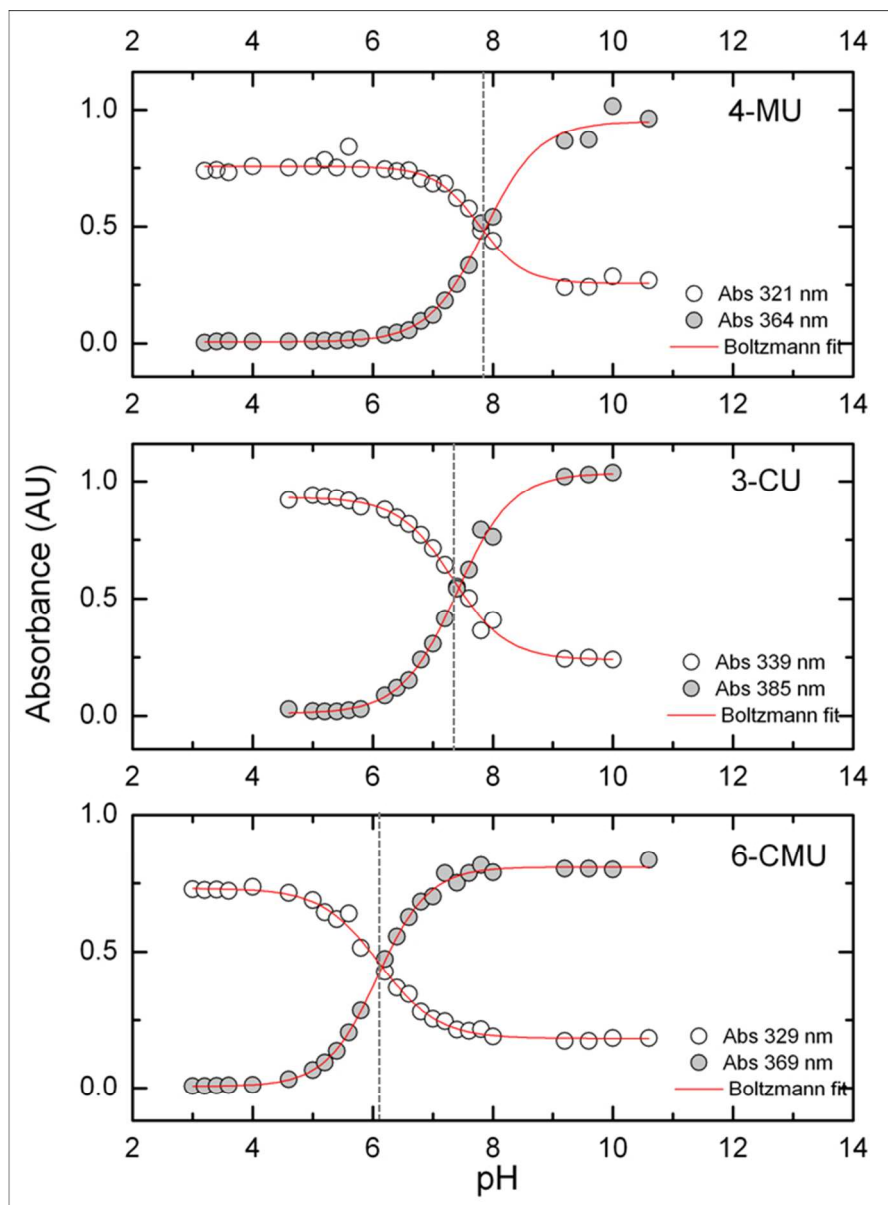


Figure 2
127x172mm (150 x 150 DPI)

1
2
3
4
5
6
7
8
9
10
11
12
13
14
15
16
17
18
19
20
21
22
23
24
25
26
27
28
29
30
31
32
33
34
35
36
37
38
39
40
41
42
43
44
45
46
47
48
49
50
51
52
53
54
55
56
57
58
59
60

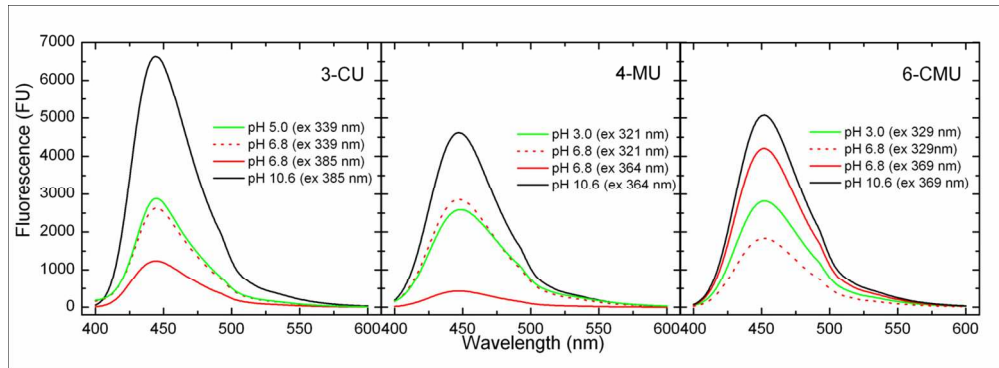


Figure 3
254x92mm (150 x 150 DPI)

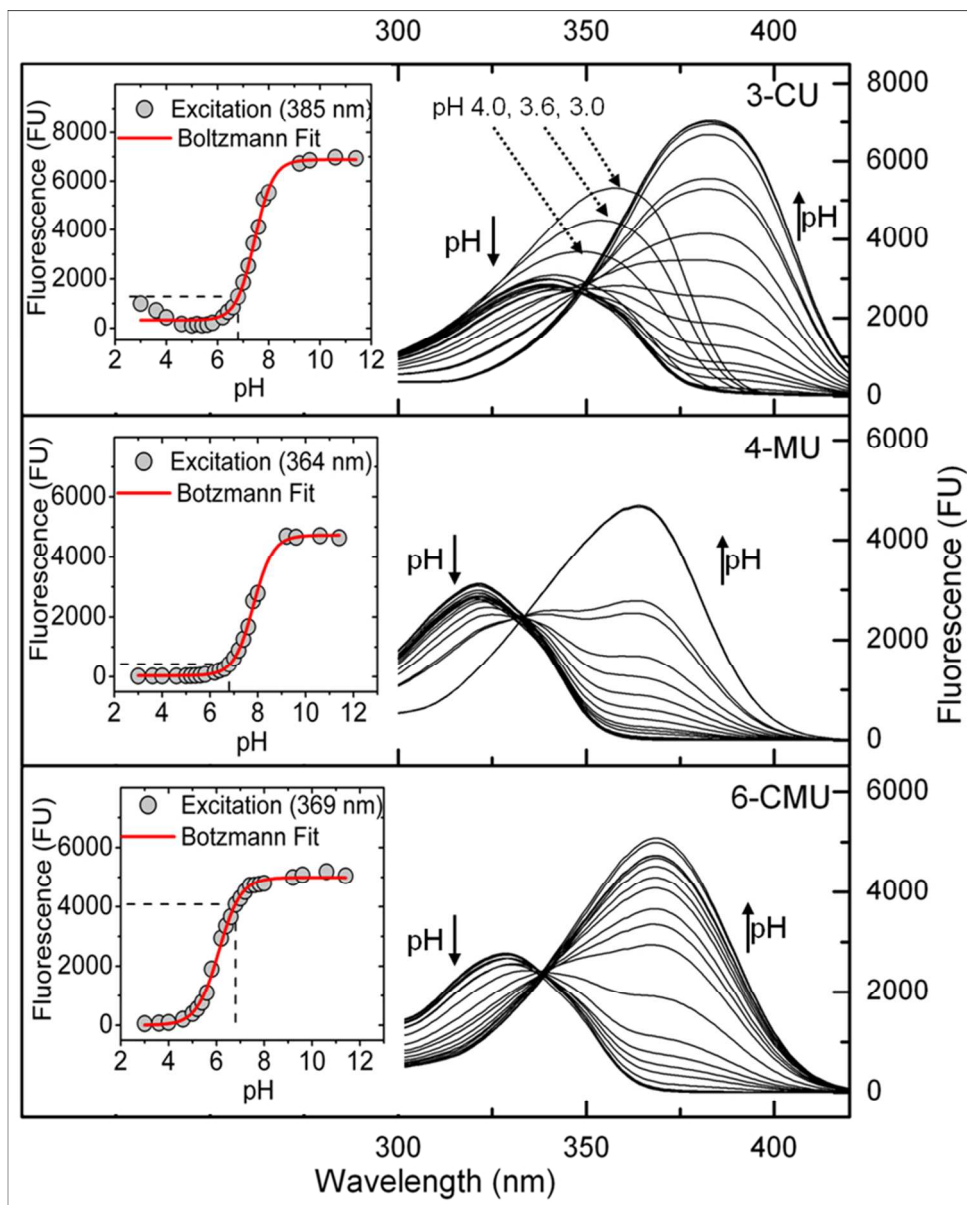


Figure 4
154x190mm (150 x 150 DPI)

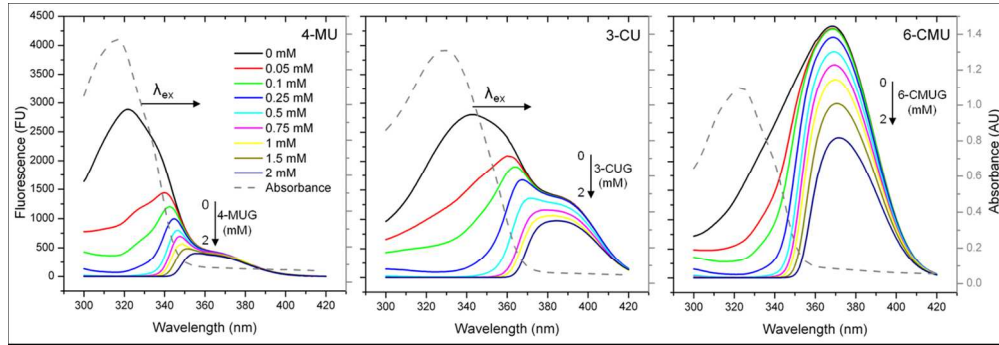


Figure 5
254x86mm (150 x 150 DPI)

1
2
3
4
5
6
7
8
9
10
11
12
13
14
15
16
17
18
19
20
21
22
23
24
25
26
27
28
29
30
31
32
33
34
35
36
37
38
39
40
41
42
43
44
45
46
47
48
49
50
51
52
53
54
55
56
57
58
59
60

1
2
3
4
5
6
7
8
9
10
11
12
13
14
15
16
17
18
19
20
21
22
23
24
25
26
27
28
29
30
31
32
33
34
35
36
37
38
39
40
41
42
43
44
45
46
47
48
49
50
51
52
53
54
55
56
57
58
59
60

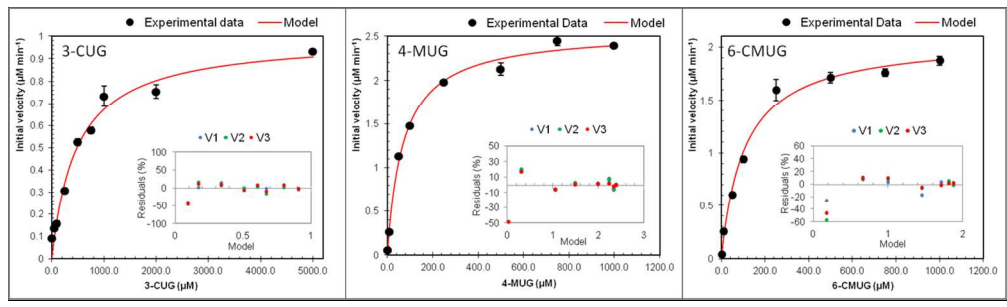


Figure 6
254x74mm (150 x 150 DPI)

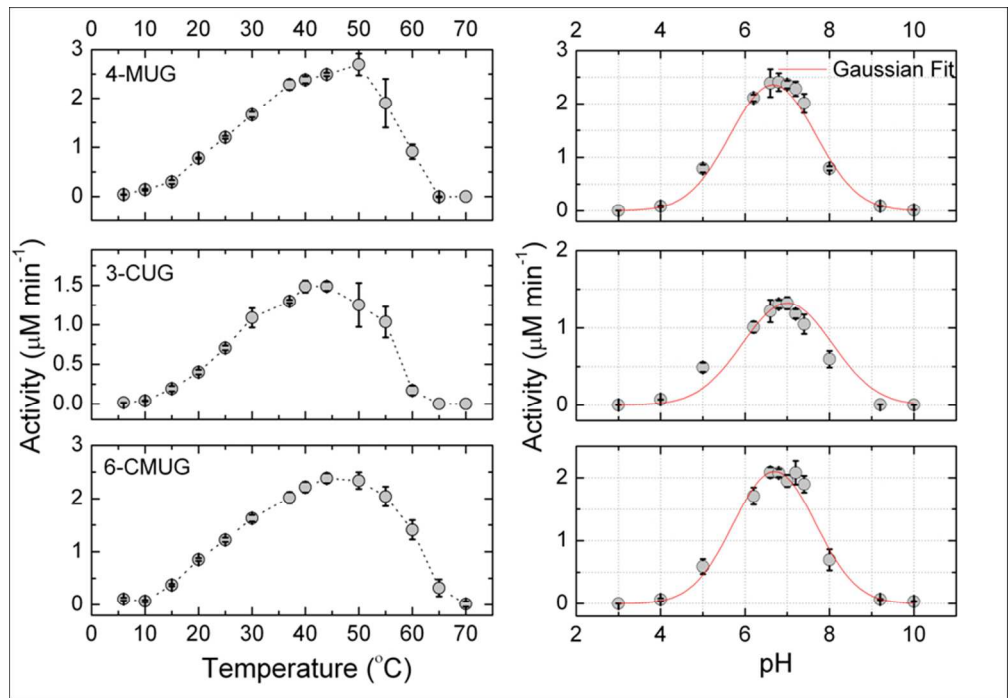


Figure 7
162x112mm (150 x 150 DPI)

1
2
3
4
5
6
7
8
9
10
11
12
13
14
15
16
17
18
19
20
21
22
23
24
25
26
27
28
29
30
31
32
33
34
35
36
37
38
39
40
41
42
43
44
45
46
47
48
49
50
51
52
53
54
55
56
57
58
59
60

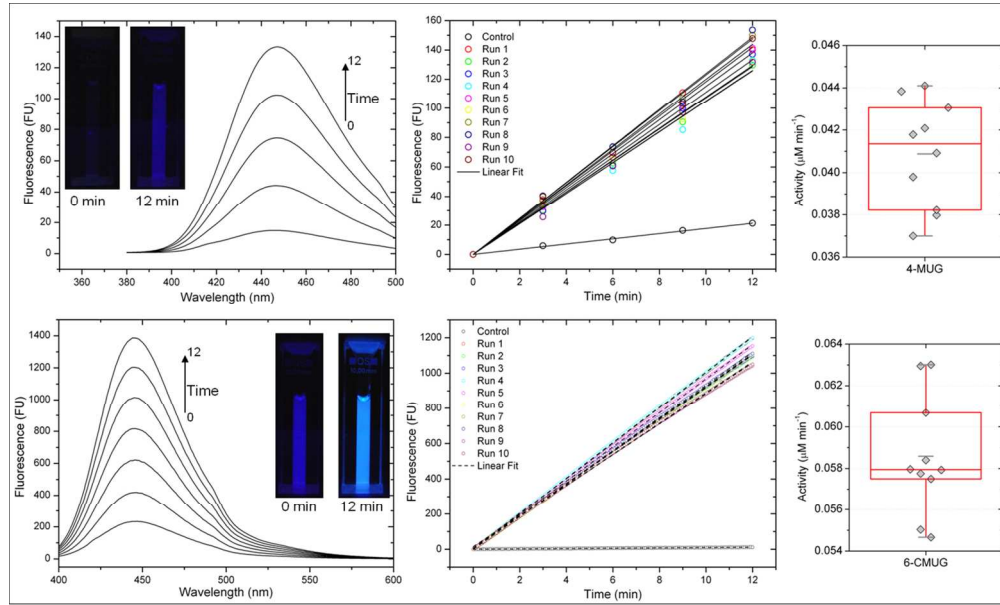


Figure 8
254x152mm (150 x 150 DPI)

1
2
3
4
5
6
7
8
9
10
11
12
13
14
15
16
17
18
19
20
21
22
23
24
25
26
27
28
29
30
31
32
33
34
35
36
37
38
39
40
41
42
43
44
45
46
47
48
49
50
51
52
53
54
55
56
57
58
59
60